Electrical-thermal performance of a cooled RF applicator for hepatic ablation with additional distant infusion of hypertonic saline: In vivo study and preliminary computer modeling

RICARDO ROMERO-MÉNDEZ[1], PILAR TOBAJAS[2], FERNANDO BURDÍO[3], ANA GONZALEZ[4], ANA NAVARRO[5], LUIS GRANDE[3], & ENRIQUE BERJANO[6]

[1] Facultad de Ingeniería, Universidad Autónoma de San Luis Potosí, San Luis Potosí, SLP, Mexico, [2] Department of Radiology, Hospital Clínico Universitario Lozano Blesa, Zaragoza, Spain, [3]Department of Surgery, Hospital del Mar, Barcelona, Spain, [4]Department of Animal Pathology and Surgery, University of Zaragoza, Spain, [5]Department of Surgery A, Hospital Clínico Universitario Lozano Blesa, Zaragoza, Spain, [6]Biomedical Synergy, Electronic Engineering Department, Universitat Politècnica de València, València, Spain

Correspondence: Dr. Enrique J. Berjano, Departament d'Enginyeria Electrònica, Universitat Politècnica de Valencia, Camí de Vera, 46022 València, Spain Email: eberjano@eln.upv.es

Abstract

Purpose: The Cool-tip electrode is one of the most widely employed applicators in radiofrequency (RF) hepatic ablation. Previous research demonstrated that it is possible to enlarge coagulation volume when the single cooled electrode is associated with distant infusion of saline (hybrid applicator). The aim of this study was to compare the electrical-thermal behavior of Cool-tip electrode with that of the hybrid applicator.

Materials and methods: Forty-two RF ablations were performed on a total of 10 pigs: 22 with the Cool-tip electrode and 20 with the hybrid applicator (low infused saline volumetric flow rate of 6 mL/h at 2 mm distance). We compared both electrical performance (delivered power and number of roll-offs, i.e. sudden rises in impedance that interrupts the power delivery) and coagulation zone characteristics. In addition, we built a one-dimensional model to provide a basic physical explanation of the difference in performance between the different applicators.

Results: The experimental results showed that the number of roll-offs with the Cool-tip electrode was higher (24.3±3.1 vs. 6.7±7.0). The hybrid applicator created larger coagulation volumes (19.7±9.5 vs. 9.5±5.8 cm^3) with larger transverse diameters (2.5±0.6 vs. 1.9±0.5 cm). The one-dimensional model confirmed the delay in the incidence of the first roll-off, but not the heterogeneity of the hybrid applicator's electrical performance in the experiments.

Conclusions: The hybrid applicator produces fewer roll-off episodes than the Cool-tip electrode and creates larger coagulation volumes with larger transverse diameters.

Keywords: cool-tip electrode, computer modeling, hepatic ablation, hybrid applicator, wet electrode, radiofrequency ablation, RF applicator, saline infusion, tumor ablation.

Introduction

Radiofrequency (RF) ablation of hepatic tumors is a current minimally invasive procedure to treat primary and metastatic liver tumors. The Cool-tip electrode (Valleylab, Boulder, CO, USA) is one of the most frequently employed applicators for RF hepatic ablation and provides reliable geometry of coagulation zones [1,2]. It consists of a single needle (i.e. electrode) with active tip of 1, 2 or 3 cm in length, or of a cluster applicator comprising three single electrodes placed close together with 2.5 cm active tips. Inside the electrode, water is circulated in a closed circuit to cool the tissue around the electrode and prevent tissue charring [3]. According to the terminology of The International Working Group of Image-Guided Tumor ablation [4] it is an *internally cooled electrode* or simply *cooled electrode*. In a previous ex vivo research we studied the effect of associating the cooled electrode with interstitial hypertonic infusion (20% NaCl) in the tissue [2]. The results showed that the optimum distance between the outlet of the infusion tube and surface of the cooled electrode was around 2 mm, which allowed larger coagulation volumes to be created than other distances (0 and 4 mm). Delivered power was also higher at this distance. With this idea in mind, we later assessed the performance of a hybrid applicator based on a cooled electrode combined with a 0.65 mm outer diameter tube that infuses saline at 2 mm from the surface of the cooled electrode, as shown in Figure 1. This assessment, based on an in vivo experimental model, was conducted by comparing the hybrid applicator to a cluster of three cooled electrodes [5]. Although both coagulation volume and minimum transverse diameter were significantly larger with the hybrid applicator, in all these previous studies the hybrid applicator employed an infusion rate of 100 mL/h, which is considered as a “higher infusion rate” (over 30 mL/h). These rates have been associated with distortions of coagulation shape [3] (i.e. complex asymmetric coagulation shapes),

or even higher rates of complications that have been linked to saline reflux along the applicator path [6,7]. To counteract this effect, other new devices employ empirically "low saline volumetric flow rates" (less than 12 mL/h) [6], like the "StarBurst Xli-enhanced" (RITA Medical Systems, AngioDynamics, Queensbury, NY, USA), which are credited with avoiding these complications.

We thus conducted an in vivo experimental study to compare the performance of the hybrid applicator at a low saline volumetric flow rate of 6 mL/h (safe saline infusion) to a single Cool-tip electrode. The results suggested that the hybrid applicator could increase coagulation zone volume without reducing predictability [8]. The current study is a complementary assessment of that study. Firstly, we studied in detail the electrical performance of both applicators and their possible correlation with coagulation zone volumes. Secondly, we built a one-dimensional theoretical model whose objective was not to reproduce in detail the electrical performance found in the experiments, but to provide a possible physical explanation of the difference in performance between the applicators.

Materials and methods

Experimental study

The experimental setup has been previously described in [8]. Briefly, all the RF ablations were conducted with a CC-1 generator (Radionics, Burlington, MA, USA). Two experimental groups were considered, one for each RF applicator: Group A used a single Cool-tip electrode of 14 gauge diameter and 3 cm in length (Valleylab, Boulder, CO, USA), while Group B employed a new hybrid applicator consisting of a single internally-cooled electrode (similar to the Cool-tip electrode) and two extendable insulated tubes (0.65 mm outer diameter) located inside the single large diameter

electrode, and through which the hypertonic (20% NaCl) saline was injected into the tissue at a volumetric flow rate of 6 mL/h (see Fig. 1). These two extendable tubes are located on the same plane and inject the saline in opposite directions. A flow rate of 20 mL/min was used to internally cool the electrode with 5ºC saline (in both applicators). A total of 42 RF ablations were analyzed: 22 with the Cool-tip electrode (Group A) and 20 with the hybrid applicator (Group B). Both applicators used a monopolar RF power delivery mode for 12 minutes with the generator set to deliver maximum power in the impedance control mode (pulsed algorithm method) [8]. This method allows the maximum power to be delivered until impedance rises to 20 Ω above the baseline value (roll-off phenomenon). At this point the power is switched off automatically to avoid a further local temperature increase. Fifteen seconds later, the power automatically switches on again. This pulsed algorithm has been demonstrated to improve coagulation volume and deposited power [9]. During each ablation the instantaneous value of the following electrical variables were recorded: voltage, current, power and impedance. Once the ablation finished, we calculated the mean power (P_m) of each ablation as:

$$P_m = \frac{1}{T_{total}} \int_0^{T_{total}} P(t)\, dt \qquad (1)$$

where $P(t)$ is the instantaneous power and T_{total} is the total duration of the ablation (720 s). We also defined the delivered energy (E) as $E = P_m \cdot T_{total}$. Due to using a pulsed algorithm, there is a 15-second switch-off period after each roll-off, during which the instantaneous power falls to zero. For this reason, we additionally defined the modified mean power (P_m*) as:

$$P_m^* = \frac{1}{T_{total} - \gamma \cdot 15} \int_0^{T_{total}} P(t)\, dt \qquad (2)$$

where γ is the number of roll-offs. This P_m* represents the mean power without considering the switch-off periods and could provide information about how RF electrical power is actually delivered, i.e. how much electrical power is delivered by the generator.

Although up to five different methods of assessing coagulation zone volume were employed in the previous study [8], here we only considered macroscopic assessment without digital reconstruction by using the ‘‘white zone’’, which is generally accepted as coagulation necrosis [4]. The so-called ‘‘red zone’’ was excluded from the measurements. The liver was first sectioned along the needle axis by cutting next to the needle surface. We assumed that this axis corresponded basically to the longitudinal axis of the coagulation zone (*a* diameter or axial diameter). Additional cuts were then made orthogonally in order to measure the two transverse diameters perpendicular to the applicator axis (*b* and *c* diameters). The three diameters (*a*, *b* and *c*) were measured in each RF ablation by consensus of two observers. Volume (ς) was then calculated as $(1/6)\cdot\pi\cdot a\cdot b\cdot c$ (volume of an ellipsoid).

Variables were compared and correlated among groups. The Kolmogorov-Smirnov test was used to determine whether values followed a normal distribution. Student's t-test and the Mann-Whitney U test analyzed mean values. Linear regression analysis was also modeled to study deposited energy. In this regard, coefficient of determination (η^2) was provided as goodness-of-fit when any significance was detected. All variables were found to be significant at a threshold of $p<0.05$. Statistical analyses were performed with SPSS version 17.0 (SPSS, Chicago, IL) statistical software.

Theoretical modeling

In order to study the effect of saline infusion into the tissue during the application of RF current, we developed a one-dimensional model that considers an internally-cooled cylindrical electrode. At a certain distance from the metallic probe there is an outlet corresponding to the tip of the extendable insulated tube that supplies a flow of saline into the tissue (see Fig. 2). This saline solution is assumed to reach tissue temperature at the needle outlet (see Section I of the supplementary file). The fluid that leaves the tube flows radially outward, infusing the tissue at a distance from the outlet. As an approximation to the central part of the device we assumed a one-dimensional flow of saline and a one dimensional variation of the temperature and voltage within the tissue. Since the cooled electrode has a length of 3 cm, here we consider that, as a rough approximation aimed at explaining the differences in electrical-thermal performance between the Cool-tip electrode and the hybrid applicator, the saline affects the central half of the device. The inner radius of the computational domain is equal to the radius of the device, r_i =1.5 mm, the outer radius is at a sufficient distance from the device, r_∞ = 60 mm. We assume that the infused saline is uniformly distributed along the length analyzed, so that the velocity is uniform at a given radius.

Realistic modeling of the hybrid applicator should include a three-dimensional structure with two extendable tubes for infusion of hypertonic saline. However, the proposed model is a simplification of the real physical situation and should therefore be considered as a preliminary study of the electrical-thermal performance of the hybrid applicator. Moreover, although the model has a simple one-dimensional geometry, it includes all the elements required to realistically model the electrical and thermal phenomena involved in RF ablation with the new hybrid applicator: 1) the thermal

convective phenomenon due to infusion of hypertonic saline into the tissue, 2) the electrical conductivity gradient around the tip of the extendable tubes due to the infusion of saline, and 3) re-hydration of the tissue desiccated by the saline. In fact, the idea of this model is to assess the ability of the saline to modify the temperature field in the tissue and to delay roll-off caused by increased impedance due to overheating of the tissue, and hence to give a physical explanation of the experimental results.

The equations to be solved are the Laplace equation for the electrical problem and the Bioheat equation with an additional convective term for the thermal problem. Section II of the supplementary file provides further details of these governing equations and tissue characteristics. The attempt to model the spatial-time distribution of tissue electrical conductivity $\sigma_T(r,t)$ and its evolution during heating was considered to be important in the theoretical study. This was estimated by considering the findings of a previous experimental study in which we tracked the saline by X-ray computed tomography during saline infusion using a healthy ex vivo porcine liver at 0.1 mL/min for 300 s [10]. Although the most important finding in this study was the strong heterogeneity of the saline-infused spatial distribution, we obtained a linear regression analysis between the mean percentage of grayscale intensity *(MPGI)* during infusion (which we assumed to be related to the percentage of saline-infused tissue), the time (t) in seconds, and the radial distance from the infusion needle in mm (d):

$$MPGI = 2.5 + 0.003 \times t - 0.98 \times d \qquad (\eta^2 = 0.3,\ p<0.0001) \qquad (3)$$

By considering this equation and the electrical conductivities of non-infused liver (σ_{np}) and 20% NaCl solution ($\sigma_{20\%}$), we were able to propose, as a first approximation, an estimate for the time-spatial distribution of electrical conductivity $\sigma_T(r,t)$ around the infusing point:

$$\sigma_T(r,t) = \sigma_{np} + [2.5 - 0.98(3 - r) + 0.003t)]\frac{1}{100}\sigma_{20\%} \qquad \text{for r < 3 mm} \quad (4)$$

$$\sigma_T(r,t) = \sigma_{np} + [2.5 - 0.98(r - 3) + 0.003t)]\frac{1}{100}\sigma_{20\%} \qquad \text{for r > 3 mm} \quad (5)$$

with $\sigma_T > \sigma_{np}$, and r in mm. If we consider values for non-infused liver σ_{np} = 0.148 S/m [11] and $\sigma_{20\%}$ = 4 S/m [12], and we consider the infusion point at, r = 3.0 mm, i.e. 1.5 mm away from the electrode surface, the time-spatial variation of the electrical conductivity due to saline-infusion is represented in Fig. 3, in which we used Equations (4 and 5) but kept $\sigma_T(r,t)$ above the value of the non-saline-perfused tissue (0.148 S/m).

Computer simulations were conducted to analyze the tissue temperature evolution and electrical impedance. Although the problem is essentially three-dimensional, the objective is not to reproduce exactly the same performance as in the experiments, but rather to explore the physical concept of saline infusion into the tissue, for which a one-dimensional approximation to the problem is plausible. The mathematical formulation of the problem and employed numerical method are described in Sections III and IV, respectively, of the supplementary file.

Results

Experimental results

The number of roll-offs in Group A was 24.3 ± 3.1 vs. 6.7 ± 7.0 in Group B ($p<0.001$) (see Table I). In fact, 45% of cases showed two or less roll-offs in Group B. In this group, there was one case with 24 roll-offs and 30% of cases had between 10 and 20. Moreover, in Group A, the roll-offs appeared more or less equidistantly spaced in time (see Fig. 4), while Group B showed a variety in the roll-off patterns. In some cases (30%), as shown in Fig. 5, no roll-offs occurred, and hence power and impedance

remained more or less constant throughout the ablation. In other cases (Fig. 6) a varying number of roll-offs occurred during the last stages of ablation. In certain cases roll-offs occurred from the early stages of ablation (see Fig. 7) and were more equidistantly spaced in time than in the case shown in Fig. 6.

Table I also shows the results of the electrical variables for each group. Both mean power and delivered energy were significantly higher in the hybrid applicator group: both mean power and delivered energy were ≈130% higher (55.5 ± 7.9 W vs. 129.9 ± 24.8 W; and 39.8 ± 5.7 kJ vs. 91.9 ± 18.9 kJ).The modified mean power was also 37% higher with the hybrid applicator (108.2 ± 11.5 W vs. 148.5 ± 10.7 W). There were no significant differences in the initial impedance between groups, although the mean value was higher for the Cool-tip electrode group (60.82 ± 18.71 Ω vs. 55.00 ±15.69 Ω).

Figure 8 shows typical views of coagulation zones created by both devices. In all cases the short coagulation necrosis diameter was one of the two transverse diameters and the largest was the axial. Coagulation zones contacted any surface of the liver (upper or lower) in 15 cases in Group A and 11 in Group B. This contact was always less than 1 cm^2 and only influenced the diameter *b* size. It should be pointed out that contact with any liver surface could limit the overall lesion volume. However, we think that limiting one diameter does not necessarily affect other diameters, since the heat lost on the target organ surface would be due to free heat convection or thermal conduction. It is therefore possible to assume there is no an automatic increase of another diameter in another direction. In fact, no limitation of the other diameters (i.e. *a* and *c*) was found in our study. No significant differences were encountered in axial diameter between the groups. However, both transverse diameters were at least 60% greater on average in Group B than Group A (Table I). An average increase of almost 50% in coagulation volume was thus observed in Group B over Group A.

Linear regression analysis between deposited energy and coagulation volume demonstrated a significant (p=0.001) but somewhat low goodness-of-fit (η^2=0.25) (Figure 9). These results were similar when mean power, corrected mean power or number of roll-offs were studied as the explanatory variable of the coagulation volume (η^2=0.24; p=0.001; η^2=0.24; p=0.001 and η^2=0.18; p=0.006, respectively). On the other hand, multivariate regression analysis combining deposited energy or any mean power with roll-off did not provide a better explanation of the variability in coagulation volume.

Computer results

Figure 10A shows the impedance evolution for both groups. The results show that saline infusion delays the appearance of the first roll-off, from 147 s (Group A) to 240 s (Group B). One of the benefits of retarding the first roll-off by saline infusion is the increased size of the lesion at this time. Figure 10B shows the temperature profiles of the tissue at roll-off for both groups. Obviously, roll-off retardation increases the size of the lesion produced in the heating period up to roll-off (the computed thermal damage, Ω=1, at that time was 21 mm with the Cool-tip electrode and 31 mm with the hybrid applicator). However, the comparison of lesion size at the end of the ablation period is more important. Fig. 11 shows the impedance evolution for 12 minutes of RF ablation computed from the theoretical model for the Cool-tip electrode (Group A) and the hybrid applicator (Group B). After the first roll-off, no difference was found in impedance evolution and the incidence of roll-offs between groups. The computed thermal damage (Ω=1) after 12 minutes ablation was 33 mm with the Cool-tip electrode and 39 mm with the hybrid applicator, which means an increase of 18% with the latter. These values correspond with the half of the larger transverse diameter.

Discussion

The experimental study was conducted to compare the electrical-thermal performance of a hybrid applicator based on distant infusion of hypertonic saline vs. a single Cool-tip electrode. The electrical behavior of the Cool-tip electrode showed higher repeatability, i.e. the progress of electrical variables (impedance and power) was more similar between ablations. This is further sustained by the fact that the hybrid applicator provides more or less three different types of behavior from an electrical point of view (Figures 5–7). These findings also suggest that distant infusion can, under certain conditions, extend the time before roll-off longer than a single Cool-tip electrode (see Fig. 4).

Additionally, we tried to assess how well electrical variables (deposited energy, mean power and number of roll-off during the procedure) predicted coagulation volume by univariate or multivariate linear regression analysis between both groups. Although all these electrical variables were shown to make a significant contribution to the final coagulation volume, the proportion of explained variability of the coagulation volume was somewhat low for deposited power, mean power or corrected mean power, whereas the number of roll-off was even lower. These data matched well with previous results from other authors, who demonstrated the predominant influence of the well known "heat sink effect" of microvascular flow over other electrical variables on the final coagulation volume when no inflow occlusion (as in the present study) occurred during RF ablation [13,14]. In other words, the cooling effect of blood flowing through large vessels (over 3 mm in diameter) in the vicinity of the ongoing ablation may be the most determinant factor in final coagulation volume and shape. Furthermore, the greater the coagulation volume the higher the probability of encountering large blood vessels,

especially in the liver dome, where a greater amount of hepatic tissue is available [15, 16]. This may account for the great variability of several hepatic ablations in bigger coagulation volumes, and for the variability found in the electrical performance.

Despite this universal limitation in RF ablation, the proposed hybrid applicator demonstrated better performance in achieving almost 50% greater coagulation volume than the simple Cool-tip electrode, even with greater coagulation volume predictability as expressed by the better coefficient of variability in coagulation volume [8]. It is also necessary to point out that this was an in vivo study on healthy pig livers with a relatively high negative influence of blood perfusion. RF ablation of tumoral tissue with different electrical and mechanical properties may therefore yield different and substantially more encouraging data.

It is also important to note that the maximum power delivered in the experiments was 100 W (the algorithm can in fact deliver even more power under some circumstances, see Fig. 5). Previous studies have suggested that the increase in tissue electrical conductivity caused by hypertonic saline infusion can increase the amount of RF energy deposited in the ablative zone, and hence the coagulation zone. However, there is a certain point at which increasing electrical conductivity can have a negative effect, as the amount of RF energy needed to heat the tissue exceeds the amount that can be administered by the generator [17,18]. In this respect, future studies should be conducted to assess the capacity of the hybrid applicator working with a higher powered generator system, as previously used with the Cool-tip electrode [19].

In addition to the experimental study, we conducted a theoretical modeling study. The objective of this study was not to reproduce the multiple roll-offs found in the experiments, but to build a model capable of explaining the longer delay in the incidence of roll-off with the hybrid applicator, as compared to a single Cool-tip

electrode. From this simplified analysis it was possible to observe that saline infusion is an effective means of retarding the appearance of the first roll-off in radiofrequency tissue heating. Since the perfused saline is entering at the surrounding tissue temperature, the delay of roll-off is not due to the cooling of the tissue by saline (as the saline exits at the surrounding tissue temperature), but has to do with the tempering effect of the phase change of the perfused saline solution on the surrounding tissue, raising this temperature to over 100°C only after the saline solution and the water content of the tissue have been completely evaporated. Increasing the retardation of roll-off also increased the area of tissue with temperature above the lethal value, so that the volume of damaged tissue was substantially higher.

The computer results of the hybrid applicator did not show the same heterogeneity in electrical performance as in the experiments (see electrical performance after first roll-off in Fig. 11). This could be due to the fact that we used a unique spatial-time distribution of electrical conductivity to model the infused tissue. This distribution was taken from experiments carried out in a previous study [10], whose most important finding was the strong heterogeneity of the spatial distribution of the infused saline. Also, in the case of a one-dimensional theoretical model, the impedance change is almost instantaneous, since the current pass is blocked once temperature reaches 100ºC. A two or three-dimensional model could probably provide a more realistic model of the physical situation by including additional paths for the electrical current, which would allow the subsequent roll-offs to be delayed when using a hybrid applicator

Conclusions

The experimental findings suggest that the hybrid applicator produces fewer roll-off episodes than the Cool-tip electrode, and creates larger coagulation volumes with longer

transverse diameters. The electrical behavior of the Cool-tip electrode showed higher repeatability, i.e. the progress of electrical variables (impedance and power) was more similar between ablations. The theoretical modeling suggests that the reason for the delay in the appearance of roll-off has to do with the heat needed to evaporate the saline solution. The one-dimensional approach was able to model the delay in the first roll-off in the case of hybrid applicator versus Cool-tip electrode, but was not able to model the heterogeneity of the hybrid applicator's electrical performance found in the experiments.

Financial support: This work received financial support from the Spanish Plan Nacional de I+D+i del Ministerio de Ciencia e Innovación grants no. TEC2008-01369/TEC and TEC2011-27133-C02-01. The authors thank CONACyT (Mexico) for support from project CB-2007/84618 that enabled research visits of R. Romero-Mendez to the Universidad Politécnica de Valencia (Spain) and E.J. Berjano to the Universidad Autónoma de San Luis Potosí (Mexico). The translation of this paper was funded by the Universitat Politècnica de València, Spain.

Author Disclosures

Drs. F Burdio and E Berjano declare an interest (stock ownership) in Apeiron Medical SL, a company which has a license for the patent application US 2010/137856 A1, on which the hybrid applicator tested in this study is based. The other authors have no conflict of interests or financial ties to disclose.

References

1. Poon RT, Fan ST, Tsang FH, Wong J. Locoregional therapies for hepatocellular carcinoma: a critical review from the surgeon's perspective. Ann Surg 2002;235:466–486.
2. Burdío F, Berjano EJ, Navarro A, Burdío JM, Güemes A, Grande L, et al. RF tumor ablation with internally cooled electrodes and saline infusion: what is the optimal location of the saline infusion? Biomed Eng Online 2007 Jul 16;6:30.

3. Pereira PL, Trübenbach J, Schenk M, Subke J, Kroeber S, Schaefer I, et al. Radiofrequency ablation: in vivo comparison of four commercially available devices in pig livers. Radiology 2004;232:482–490.

4. Goldberg SN, Grassi CJ, Cardella JF, Charboneau JW, Dodd 3rd GD, Dupuy DE, et al. Image-guided tumor ablation: standardization of terminology and reporting criteria. Radiology 2005;235: 728–739.

5. Burdio F, Navarro A, Berjano EJ, Burdío JM, Gonzalez A, Güemes A, et al. Radiofrequency hepatic ablation with internally cooled electrodes and hybrid applicators with distant saline infusion using an in vivo porcine model. Eur J SurgOncol 2008;34:822–830.

6. Gillams AR, Lees WR. CT mapping of the distribution of saline during radiofrequency ablation with perfusion electrodes. Cardiovasc Intervent Radiol 2005;28:476–480.

7. Kettenbach J, Köstler W, Rücklinger E, Gustorff B, Hüpfl M, Wolf F, et al. Percutaneous saline-enhanced radiofrequency ablation of unresectable hepatic tumors: initial experience in 26 patients. AJR Am J Roentgenol 2003;180:1537–1545.

8. Burdío F, Tobajas P, Quesada-Diez R, Berjano E, Navarro A, Poves I, et al. Distant infusion of saline may enlarge coagulation volume during radiofrequency ablation of liver tissue using cool-tip electrodes without impairing predictability. AJR Am J Roentgenol. 2011 Jun;196(6):W837-43.

9. Goldberg SN, Stein MC, Gazelle GS, Sheiman RG, Kruskal JB, Clouse ME. Percutaneous radiofrequency tissue ablation: optimization of pulsed-radiofrequency technique to increase coagulation necrosis. J Vasc Interv Radiol 1999;10:907–916.

10. Burdío F, Berjano E, Millan O, Grande L, Poves I, Silva C, et al. CT mapping of saline distribution during injection into the liver in several image-guided procedures: how much tissue is actually infused? An ex vivo pig liver study. Physica Medica, 2012, at press.

11. Chang I. Finite element analysis of hepatic radiofrequency ablation probes using temperature-dependent electrical conductivity. Biomed Eng Online. 2003 May 8;2:12.

12. Aubé C, Schmidt D, Brieger J, Schenk M, Kroeber S, Vielle B, et al. Influence of NaCl concentrations on coagulation, temperature, and electrical conductivity using a perfusion radiofrequency ablation system: an ex vivo experimental study. Cardiovasc Intervent Radiol. 2007 Jan-Feb;30(1):92-7.

13. Goldberg SN, Hahn PF, Tanabe KK, Mueller PR, Schima W, Athanasuolis CA, et al. Percutaneous

radiofrequency tissue ablation: does perfusion-mediated tissue cooling limit coagulation necrosis? J Vasc Interv Radiol 1998;9;1–11.

14. Patterson EJ, Scudamore CH, Owen DA, Nagy AG, Buczkowski AK. Radiofrequency ablation of porcine liver in vivo. Effects of blood flow and treatment time on lesion size. Ann Surg 1998;227:559–565.

15. Thein E, Becker M, Anetzberger H, Hammer C, Messmer K. Direct and distribution of regional portal blood flow in the pig by means of fluorescent microspheres. J Appl Physiol 2003;95:1808–1816.

16. Dondelinger RF, Ghysels MP, Brisbois D, Donkers E, Snaps FR, Saunders J, et al. Relevant radiological anatomy of the pig as a training model in interventional radiology. Eur Radiol 1998;8:1254–1273.

17. Lobo SM, Afzal KS, Ahmed M, Kruskal JB, Lenkinski RE, Goldberg SN. Radiofrequency ablation: modeling the enhanced temperature response to adjuvant NaCl pretreatment. Radiology. 2004 Jan;230(1):175-82.

18. Lobo SM, Liu ZJ, Yu NC, Humphries S, Ahmed M, Cosman ER, et al. RF tumour ablation: computer simulation and mathematical modelling of the effects of electrical and thermal conductivity. Int J Hyperthermia. 2005 May;21(3):199-213.

19. Solazzo SA, Ahmed M, Liu Z, Hines-Peralta AU, Goldberg SN. High-power generator for radiofrequency ablation: larger electrodes and pulsing algorithms in bovine ex vivo and porcine in vivo settings. Radiology. 2007 Mar;242(3):743-50.

Table I. Electrical parameters and coagulation volumes. Values correspond to mean ± standard deviation.

	Group		
	A: Cool-tip electrode (n = 22)	B: Hybrid applicator (n = 20)	*p*-value
Number of roll-offs	24.3 ± 3.1	6.7 ± 7.0	0.002
P (W)	55.5 ± 7.9	129.9 ± 24.8	<0.001
E (kJ)	39.8 ± 5.7	91.9 ± 18.9	<0.001
*P** (W)	108.2 ± 11.5	148.5 ± 10.7	<0.001
ς (cm^3)	9.5 ± 5.8	19.7 ± 9.5	0.002
a diameter (cm)	3.7 ± 1.0	4.2 ± 1.5	N.S.
b diameter (cm)	1.9 ± 0.5	2.5 ± 0.6	0.003
c diameter (cm)	2.3 ± 0.6	3.4 ± 1.1	0.001

P: mean power; *E*: energy; *P**: Corrected mean power (see text for details). ς: Coagulation volume; *a* diameter: axial diameter; *b* diameter: minimum transverse diameter; *c* diameter: maximum transverse diameter (see text for details). Statistically significant ($p < 0.05$). N.S: no significant difference.

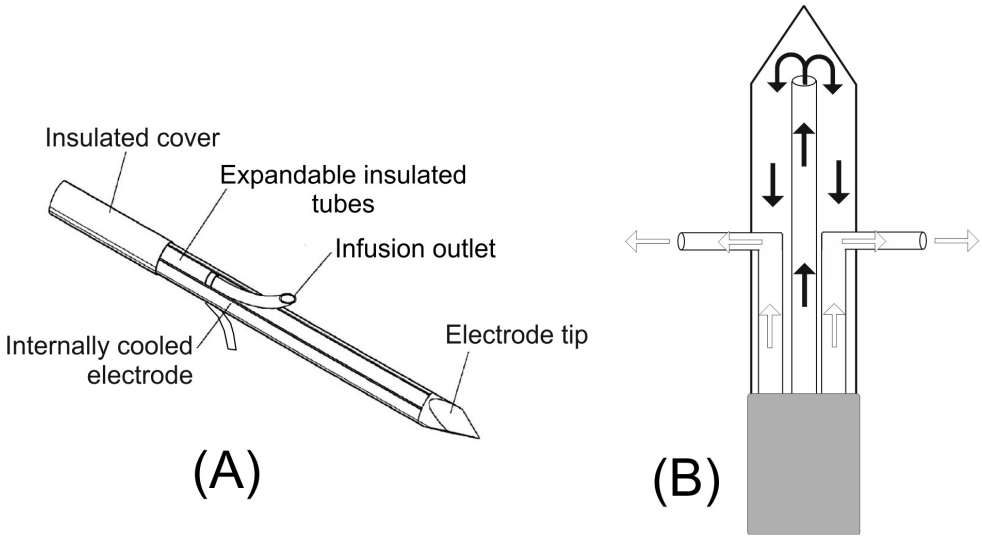

Figure 1 (A) Schematic of the hybrid applicator including a single internally cooled electrode (similar to the Cool-tip system) and two small-diameter (14 gauge) extendable insulated tubes through which the hypertonic (20% NaCl) saline is infused into the tissue at 6 mL/h. (B) Design of the hybrid applicator showing the internal coolant circulation (black arrows) and the double saline infusion circuit (white arrows).

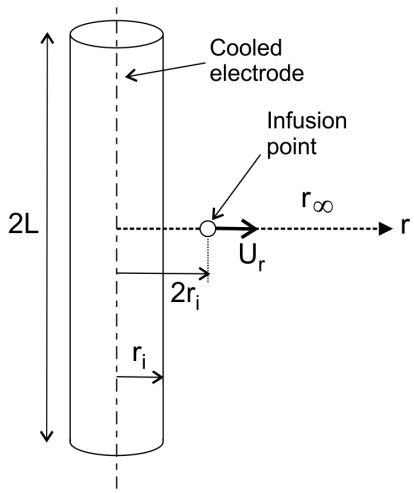

Figure 2 Schematic of the one-dimensional model (not to scale) to study the electrical-thermal performance of the hybrid applicator. The applicator has a radius r_i and it is internally cooled by a circulating fluid. At a certain distance $2r_i$, a saline solution is injected into the tissue uniformly distributed over a length $2L$=0.015 m.

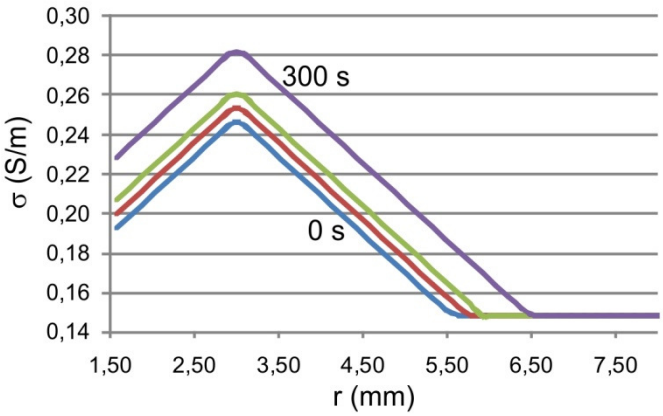

Figure 3 Spatial variation of the electrical conductivity of liver due to saline-infusion for 0, 60, 120 and 300 s (as stated in Equations (4) and (5) with $\sigma_T(r,t) \geq \sigma_{np}$). Note that the peak is located at the infusion point r = 3.0 mm, i.e. 1.5 mm away from the electrode surface and that at 0 s of RF delivery, the saline distribution corresponds to 120 seconds of infusion (saline infusion begins 2 minutes before power deposition).

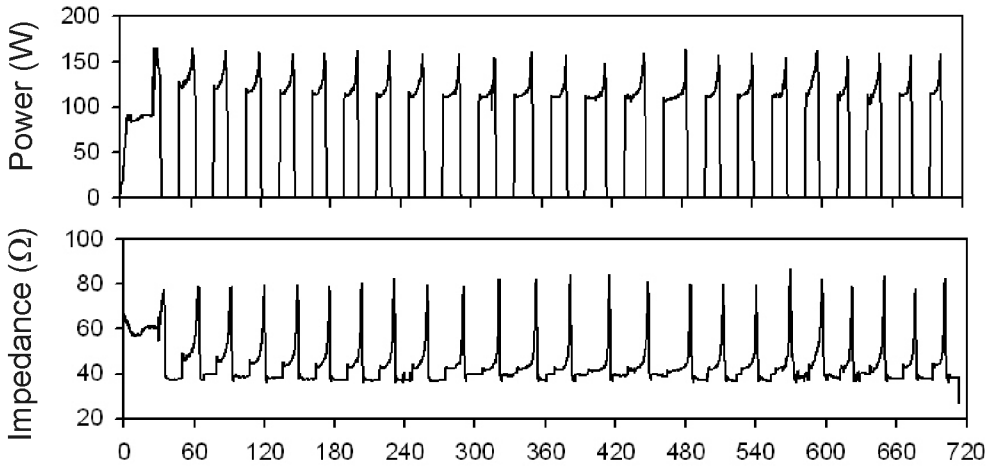

Figure 4 Typical progress of power and impedance throughout a 12-minute ablation with a single Cool-tip RF applicator. Note that roll-offs (rapid increase of impedance and subsequent drop in applied power) appear more or less equidistantly spaced in time.

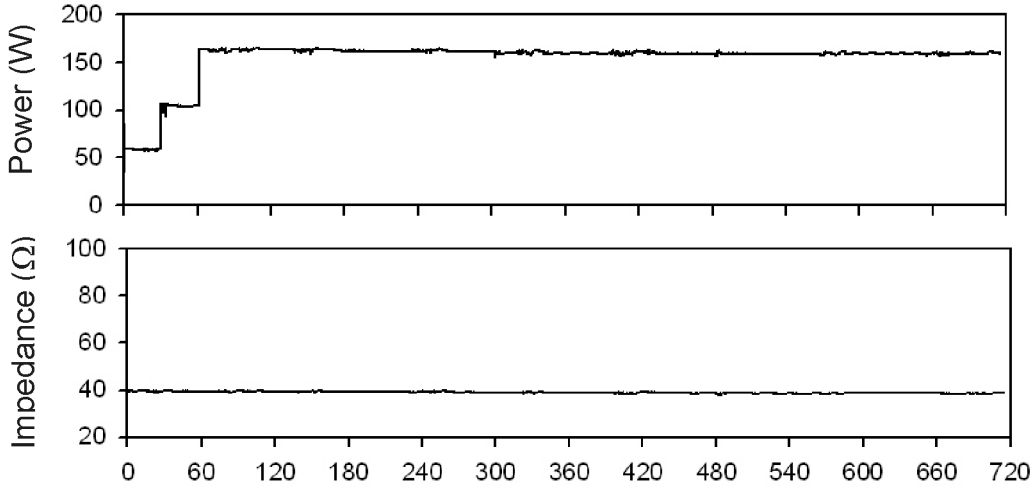

Figure 5 Progress of power and impedance throughout a 12-minute ablation with the hybrid applicator. In this experiment there were no roll-offs. 45% of ablations showed two or less roll-offs.

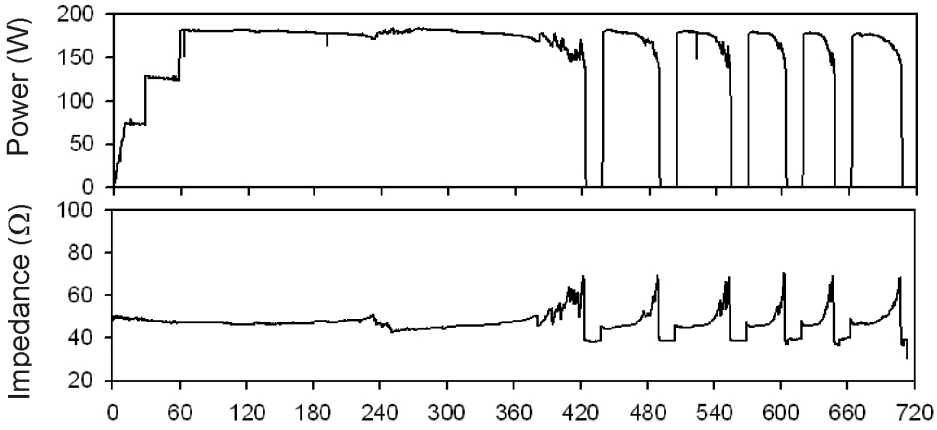

Figure 6 Progress of power and impedance throughout a 12-minute ablation with the hybrid applicator. This experiment showed six roll-offs occurred during the last 4 minutes of ablation. The result suggests that from this time on the hybrid applicator behaved similarly to a single Cool-tip electrode, but with roll-offs more spaced in time and higher deposited power than the Cool-tip electrode.

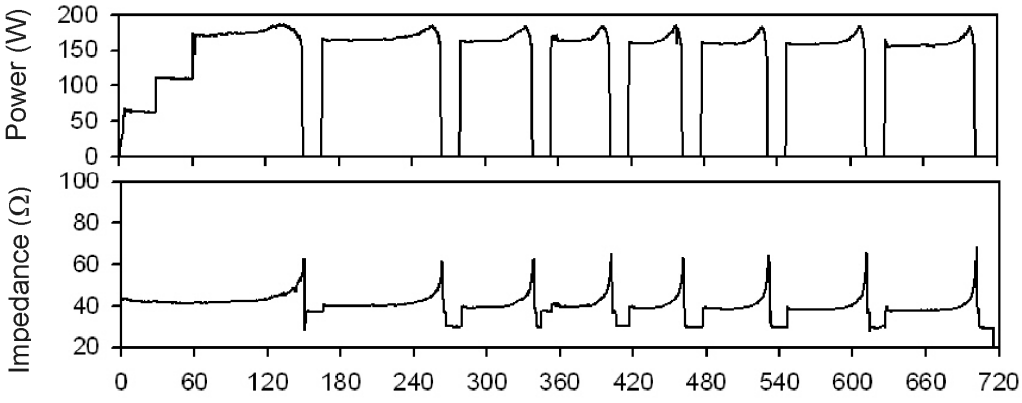

Figure 7 Progress of power and impedance throughout a 12-minute ablation with the hybrid applicator. This experiment showed eight roll-offs distributed more evenly across the course of the 12-minutes ablation than in the case of Fig. 5, which suggests that distant infusion could delay roll-offs and

give higher deposited power compared to the case of a single Cool-tip electrode.

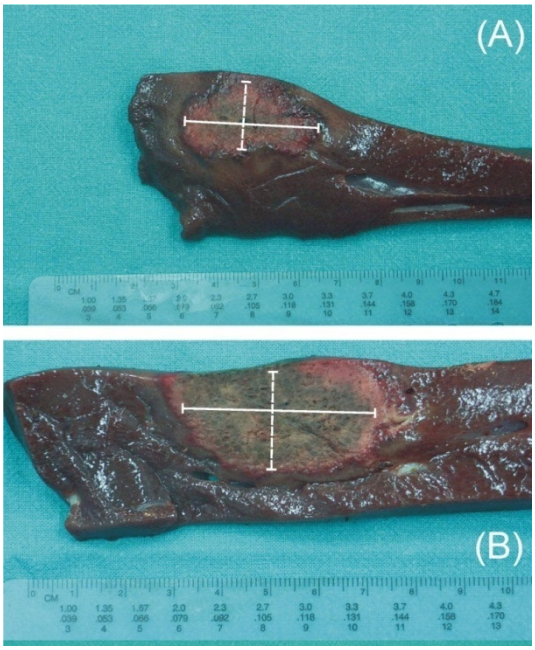

Figure 8 Coagulation zones produced by the Cool-tip electrode (A) and hybrid applicator (B). The ‘‘white zone’’ was used as coagulation necrosis zone. Since the livers were cut into slices of 1 cm along the axis of the electrode, the photos show the axial plane. Two diameters of the coagulation zone are shown: the solid line is the diameter along the applicator track (i.e. *a* diameter or axial diameter); and the dashed line is one of the two transverse diameters, height assessed perpendicular to axial diameter and to liver surface.

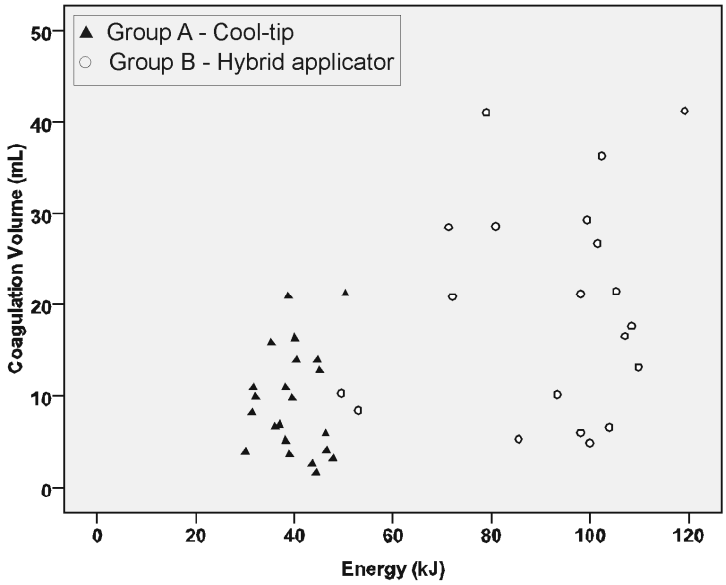

Figure 9 Scatter plot of linear relationship between deposited energy (kJ) and coagulation volume in Group A-Cool-tip electrode (triangles) and Group B-hybrid applicator (circles). The greater the energy to be deposited the greater the coagulation volume (η^2=0.25; p=0.001) but variability increases with higher amounts of deposited energy (especially evident in Group B).

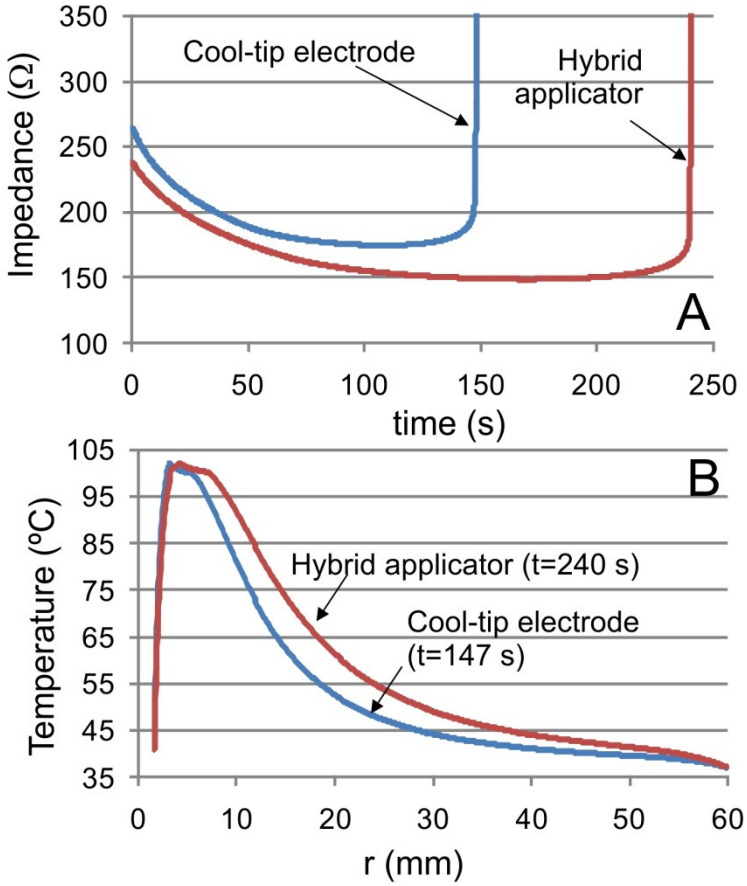

Figure 10 Impedance evolution (A) and temperature profiles at roll-off (B) for the Cool-tip electrode (Group A) and the hybrid applicator (Group B) computed from the theoretical model.

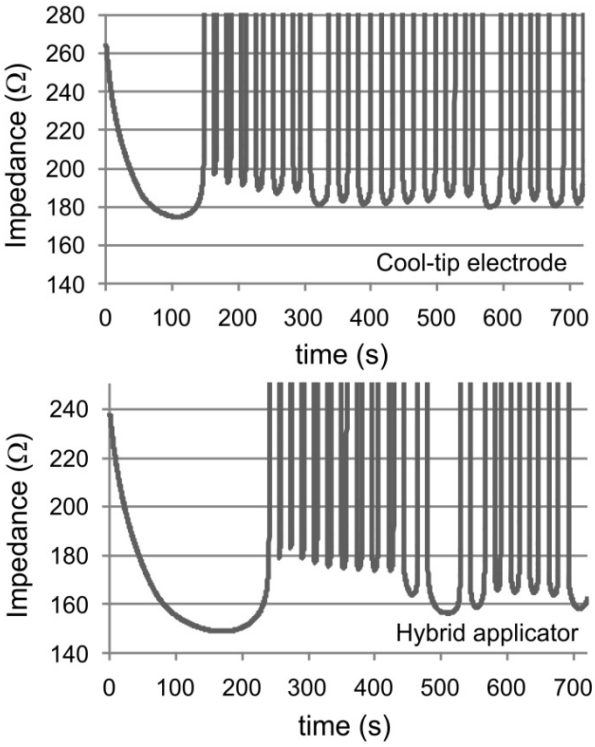

Figure 11 Impedance evolution for 12 minutes of RF ablation computed from the theoretical model for the Cool-tip electrode (Group A) and the hybrid applicator (Group B).